Title

Development of a Biotinylated Nanobody-Based Gold Nanoparticle Immunochromatographic Assay for the Detection of Procymidone in Crops

Journal

Journal of Agricultural and Food Chemistry, 71(35)

ISSN

0021-8561

Authors

Liu, Min-Ling

He, Xiao-Ting

Xu, Zhen-Lin

et al.

Publication Date

2023-09-06

DOI

10.1021/acs.jafc.3c03408

Peer reviewed

HHS Public Access

Author manuscript

J Agric Food Chem. Author manuscript; available in PMC 2024 September 06.

Published in final edited form as:

J Agric Food Chem. 2023 September 06; 71(35): 13137–13146. doi:10.1021/acs.jafc.3c03408.

Development of a Biotinylated Nanobody-based Gold Nanoparticle Immunochromatographic Assay for the Detection of Procymidone in Crops

Min-Ling Liu[a,1], **Xiao-Ting He**[a,1], **Zhen-Lin Xu**[a], **Hao Deng**[b], **Yu-Dong Shen**[a], **Lin Luo**[a], **Xing Shen**[a], **Zi-Jian Chen**[c,*], **Bruce Hammock**[d], **Hong Wang**[a,*]

[a]Guangdong Provincial Key Laboratory of Food Quality and Safety, South China Agricultural University, Guangzhou 510642, China.

[b]Key Laboratory of Tropical Fruit and Vegetable Cold-chain of Hainan Province / Institute of Agro-products Processing and Design, Hainan Academy of Agricultural Sciences, Haikou, 570100, China

[c]Laboratory of Quality & Safety Risk Assessment for Agro-products (Zhaoqing), Ministry of Agriculture and Rural Affairs, School of Food and Pharmaceutical Engineering, Zhaoqing University, Zhaoqing, 526061, China

[d]Department of Entomology and UCD Comprehensive Cancer Center, University of California, Davis, California 95616, United States

Abstract

A heavy-chain antibody (VHH) library against procymidone (PRM) was constructed via immunizing *Bactrian* camel. Through careful biopanning, seven nanobodies (Nbs) with different sequences were obtained. The variability in their performance was primarily attributed to the amino acid differences in the complementarity-determining region 3 (CDR3), as analyzed by molecular docking. The Nb exhibited the highest sensitivity, named NbFM5, was biotinylated and conjugated to streptavidin-labeled gold nanoparticle to preserve the epitope's activity and prevent a decrease in sensitivity due to traditional random electrostatic adsorption. Subsequently, a simple and sensitive immunochromatographic assay (ICA) was developed for the rapid detection of PRM based on the biotinylated Nb (btNb). The developed btNb-ICA showed a cut-off value

*Corresponding author: gzwhongd@163.com (H Wang), guangdongchenzj@163.com (Z-J Chen).

[1]These authors are equally contributed to this work

Author Contribution

Min-Ling Liu: Data curation, Formal analysis, Investigation, Methodology, Writing – original draft. Xiao-Ting He: Data curation, Formal analysis, Investigation, Methodology, Writing – review & editing. Hao Deng: Data curation. Zhen-Lin Xu, Yu-Dong Shen, Lin Luo, Xing-Shen and Bruce Hammock: Investigation, Resources, Funding acquisition. Zi-Jian Chen: Writing – review & editing, Project administration. Hong Wang: Writing – review & editing, Conceptualization.

Declaration of Competing Interest

The authors declare that they have no known competing financial interests or personal relationships that could have appeared to influence the work reported in this paper.

Supporting Information

Several relative materials and methods; The amino acid sequences of colony PCR positive clones; identification of PRM positive phage via ic-ELISA; model evaluation of NbFM5 and NbFM7; cross reaction results of btNb-ICA; identification of temperature tolerance and acid-base tolerance; identification of organic tolerance; the effect of the ratio of reducing agent on the preparation of GNPs; the optimization of the dosages of GNP@btNb and PRMH-BSA; the optimization of ion concentration and pH.

of 200 ng/mL for visual judgement and a half-inhibitory concentration (IC_{50}) of 6.04 ng/mL for quantitative detection. The limit of detection (LOD) was as low as 0.88 ng/mL. The recoveries in actual samples of crops ranged from 82.2% to 117.3%, aligning well with the results obtained from GC-MS/MS (R^2=0.995). In summary, the developed btNb-ICA demonstrated high specificity and good accuracy for the rapid detection of PRM residues in vegetables. The total analysis time from preparing the sample to obtaining the result was less than 25 minutes.

Graphical Abstract

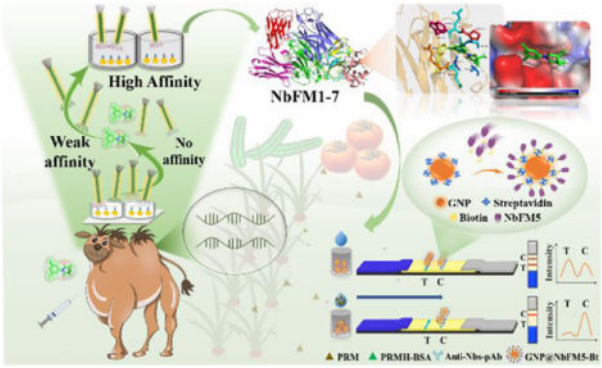

Keywords

procymidone; nanobodies; biotinylation; streptavidin; immunochromatographic assay

INTRODUCTION

Procymidone (PRM) is a fungicide with low toxicity, widely used to control botrytis cinerea and sclerotinia on crops[1]. However, there is growing concern about its high detection and over-standard rates, particularly in chives, cucumbers and tomatoes, with frequent reports of excessive levels during supervision and spot-check[2]. Of particular concern, excessive levels of PRM pose a risk to human health, potentially causing chronic toxic effects and severe kidney damage[3, 4]. Hence, strict monitoring of PRM residues is crucial for human health. Currently, many countries and organizations have established strict maximum residue limits (MRLs) for PRM in crops, including China (2 mg/kg in cucumbers/tomatoes[5], and 5 mg/kg in chives[6]), Korea (2 mg/kg in cucumbers, 5 mg/kg in chives, 10 mg/kg in tomatoes)[7], Japan (2 mg/kg in chives and 4 mg/kg in cucumbers/tomatoes)[8] and USA (5 mg/kg)[9]. Thus, it is essential to develop a more sensitive method for the rapid detection of PRM residues to prevent the harm caused by varying limit standards.

Traditional instrumental detection methods offer good reproducibility and high accuracy[10], while exhibited limitations such as complex sample pretreatment, expensive instruments and time-consuming processes. The immunoassay based on antibodies provide a sensitive, accurate, simple and rapid approach for screening pesticide residues. Despite this, there have been only a few reported cases of immunoassays for PRM using the indirect competitive enzyme-linked immunosorbent assay (ic-ELISA)[11]. Recently, nanobody (Nb) have gained interest as they exhibit several advantages, which are characterized by their low molecular

weight, high stability and high affinity. It could be obtained via the cloning of the variable domain of the heavy-chain of heavy-chain antibody (VHH) found in camels, comprising only 3 complementarity determining regions (CDRs) and 4 framework regions (FRs)[12], while maintains intact antigen-binding capacity. Notably, Nbs possess several superiorities over traditional antibodies for immunoassay methods development[13,14]. Nbs are easier to produce in large quantities, reduce production costs, and allow efficient labeling and minimal batch-to-batch variation. Additionally, their superior stability and longer storage period enable high activity under various extreme conditions. Consequently, it is widely used in the detection of small molecule pollutants at present[15].

In this study, we aimed to explore the application of highly sensitive and stable Nbs as a promising alternative method for small molecule immunochromatographic assays[16]. Our plan involved obtaining several highly specific Nbs for PRM through immunization, phage display and gene library screening. Subsequently, a gold-labeled immunochromatographic assay based on biotinylated Nb (btNb-ICA) would be established (Scheme 1). It was hopeful to expand the practical application of Nbs in rapid detection, and provide a new method for the study of ICA.

EXPERIMENTAL SECTION

Materials and Instruments.

The hapten PRMH was previously prepared by our laboratory. The details were shown in the Supporting Information (SI). The pINQ-BtH6 vector and the pCY216 vector with the BirA gene were gifts from Professor González-Sapienza Gualberto (University of the Republic of Uruguay). PRM and analogue standards were purchased from Tanmo Quality Inspection Technology Co. Ltd. (Beijing, China). DNA Engine PCR Amplifying apparatus (BIORAD, USA), Multiskan MK3 Enzyme marker (Thermo Fisher, USA), HGS510 Film Cutter (Zhejiang, China), HGS201 Cutting machine (Zhejiang, China), GIC-Q Gold label detector (Zhejiang, China). Other materials and instruments were summarized in SI.

Immunization and construction of phage display VHH library.

To prepare the immunogen and coating antigen, PRMH was covalently conjugated with Lactoferrin (PRMH-LF) and Bovine serum albumin (PRMH-BSA) following the conjugation protocols provided in SI. Then immunization was performed on a healthy alpaca (Hebei, China) using PRMH-LF. Peripheral blood mononuclear cells were isolated from fresh blood through density gradient centrifugation using lymphocyte separation medium (850 g ~ 4000 g, 4 °C, 15 ~ 25 min). Protein G affinity chromatography column was used for purification of the isolated cells[17]. Subsequently, the total RNA was extracted and immediately reverse transcribed to cDNA using a reverse transcription kit[18]. Nested PCR was performed to amplify the VHH genes and the specific primers are showed in Table S1. The target band was recovered via two rounds of amplification and the vector containing the target genes was obtained by digesting the plasmid vector pcomb3xSS by *Sfi*I and linking by T4 DNA ligase. The resulting recombinant vectors were transformed into fresh competent cell *E. coli* TG1 cells by electroporation. The transgenic cells were calculated and amplified

on an agarose medium with ampicillin. The colony PCR using Fr1-*Sfi*I and Fr4-*Sfi*I primers was performed to analyze the positive insertion rate of the gene library.

Biopanning of PRM selective phage clone.

After the gene library was obtained, a portion of cells were cultured and infected by M13KO7 helper phage to generate phage library[19]. The genes of PRM selective clones were selected by a simultaneous competition panning strategy[20] and the screening was performed by ic-ELISA. All the candidate clones were sequenced to identify their amino acid sequence. The details of the protocol were summarized in SI.

Expression and identification of the anti-PRM Nbs.

The *E. coli* BL21 (DE3) were transformed with recombinant plasmids by heat shock at 42 °C for 90 s and grown on LB plates overnight at 37 °C[21]. The positive clones were selected for the production of soluble proteins. The proteins in periplasmic lumen were extracted by cold osmotic shock method and purified using Ni-NTA resin with 200 mmol/L imidazole in 0.01 mol/L PBS for elution. To confirm the resulting anti-PRM Nbs protein, 12% SDS-PAGE and western blotting were performed. The performances of anti-PRM Nbs were further compared in ELISA detection. Finally, Molecular docking using LeadIT 2.3.2 and Pymol 2.4.0 was employed to study the recognition of VHHs to the antigen. In short, structural models of anti-PRM Nbs were built via AlphaFold2. Then the credibility of the model was confirmed by UCLA-DOE LAB-SAVES v6.0 website database (https://saves.mbi.ucla.edu/). And the molecular structure of PRM was obtained from the PubChem database (https://pubchem.ncbi.nlm.nih.gov/). Docking simulations were performed using leadit-2.3.2-Linux-x64 (http://www.biosolveit.de/LeadIT/) via Enthalpy and Entropy (hybrid approach) ligand binding setting and the others were default. Finally, the docking model with the highest score, i.e., the lowest binding free energy, was selected to analyze the interaction forces between Nbs and ligand using Open-Source PyMoLTM and LigPlus.

Preparation of biotinylated nanobody.

The Nb with highest affinity was selected. The VHH gene was amplified and ligated to pINQ-BtH6 vector containing the biotin gene by enzyme digestion and ligation[20]. The recombinant plasmid was transformed into pCY216 natural competence *E. coli* BL21(DE3). Then the btNb was expressed, purified, and identified via ELISA.

Preparation of gold nanoparticle and GNP@SA-btNb.

Gold nanoparticle (GNP) was prepared by sodium citrate method[22]. In short, 2 mL of 0.2 g/L chloroauric acid solution was added to 96, 95.5, 95, 94.5, 94 mL of ultrapure water to boiling, respectively, after heating the ultrapure water. Then 2, 2.5, 3, 3.5, 4 mL of 0.2 g/L trisodium citrate solution (the ratio of chloroauric acid to trisodium citrate was 8:8, 8:10, 8:12, 8:14, 8:16) was added, respectively, after 1 min of boiling. Subsequently, the solution changed from clear to black, and then turn to translucent burgundy within 5 min. After heating for 20 min, streptavidin labeled GNP (1 mL) was prepared by mixing it with a potassium carbonate solution (0.1 mol/L, pH8 ~ 11) and SA for 30 min, then centrifuged at 4 °C, 13400 *g* for 15 min. For the preparation of GNP@SA-btNb, btNb (2.5 mg/mL) was

incubated with GNP@SA for 30 min at room temperature, followed by purification through centrifugal washing. Finally, the GNP@SA-btNb complex was coated in 96-well plates and dried overnight at 37 °C.

Development and optimization of btNb-ICA.

The ICA was assembled with a sample pad, absorbent paper, nitrocellulose membrane (NC membrane) and PVC base plate. Then PRMH-BSA (1 mg/mL) and the secondary antibody (1.1 mg/mL) were fixed on NC membrane as the test line (T-line) and control line (C-line), respectively. The assembly was then dried at 37°C for 12 h. Finally, the NC film, sample pad and absorbent pad were assembled on the bottom plate and cut into 4 mm wide strips by a slicing instrument. To perform the assay, 100 μl of the sample solution was added to the micropores containing GNP probe to react at room temperature for 3 min. The solution was then added to the sample pad and allowed to react for 5 min. The results can be qualitatively observed with the naked eye, and the T/C value read by the reader can be used for quantitative calculations. Subsequently, various parameters and criteria were explored to find the optimal values for the test strip, including the particle size of GNPs (8:8, 8:10, 8:12, 8:14, 8:16), labeled pH (8 ~ 11), the concentration of labeled protein (btNb: 27.8 ~ 83.3 μg/mL; SA:16.2 ~ 81.1 μg/mL), the added amount of probe (10 ~ 20 μL), the concentration of PRMH-BSA (0.5 mg/mL, 1 mg/mL, 2 mg/mL) and the composition of sample pad treatment solution (PB, PBS, BB, Tris-HCl). Detailed information can be found in the SI.

Recovery test and instrumental verification.

The chives sample was subjected to pretreatment for analysis[23] by mixing with acetonitrile, shaking with some reagents and centrifuged for 5 min (1960 *g*, 16 °C). Next, the sample was mixed with anhydrous magnesium sulfate, PSA and GCB, shook for 1 min and centrifuged (1960 *g*, 16 °C, 5 min) to obtain the final sample solution. To evaluate the recovery of the method, a recovery test was conducted and compared with the analysis performed using GC-MS/MS. The details of recovery test and GC-MS/MS conditions were shown in SI.

RESULTS AND DISCUSSION

Construction of Nb genes library and Screening of Phage Display Library.

After immunizing *Bactrian* camels with PRMH-LF for 5 rounds, the antigen-binding ability and inhibitory effect of pre- and post-immunization serum were compared using ELISA (Figure 1a, b). Subsequently, RNA was extracted from the peripheral blood of immunized camels (3–5 rounds) to construct a gene library. Based on the differential binding strength to Protein G and Protein A, three different antibody subtypes were isolated from serum of the *Bactrian* camel (Figure 1c, d), including IgG_1 heavy chain (50 kDa), IgG_1 light chain (25 kDa), IgG_2 (64 kDa) and IgG_3 (43 kDa). Among these subtypes, IgG_3 was the predominant subtype in *Bactrian* camels followed by IgG_2[24]. Notably, IgG1 exhibited higher antigen binding capacity, while the inhibitory effects of the heavy chain antibodies (HcAbs) were more prominent. This suggested the generation of anti-PRM HcAbs in *Bactrian* camels and their potential utility for constructing a gene library of Nbs.

To isolate lymphocytes from peripheral blood, Trizol lysate was used for total RNA extraction. The extraction process yielded two distinct bands (28 S, 18 S) and an obscure band (5 S) (Figure 1e), with the intensity of the 28 S band being twice that of the 18S band, indicating successful and complete RNA extraction. The extracted total RNA was then reverse transcribed into cDNA using a commercial kit, followed by nested PCR amplification (Figure 1f). In the first round of PCR, the cDNA templates amplified IgG_1(1000 bp), IgG_{2a} (800 bp) and IgG_3(700 bp) (Figure 1g). From this amplification, the IgG_{2a}, IgG_3 fragments were isolated and employed as templates for the second round of PCR, producing a target VHH fragment of 500 bp using specific primers (Figure 1h). The resulting product was then digested with *Sfi*I and ligated into the digested pcom3xSS vector using T4 DNA ligase[21]. Following the transformation, the constructed plasmid was transformed into *E. coli* TG1 by electroporation and the capacity of the library was determined, yielding a library size of approximately 2.27×10^7 cfu/mL (227 individual colonies) and a positive insertion rate of 93.3% (Figure S1a), which determined through colony PCR identification. After sequencing on these positive clones, the amino acid sequence alignments were shown in Figure S1b. Notably, the number and composition of amino acids in CDR1, CDR2 and CDR3 exhibited significant variability. Furthermore, the absence of repetitive sequences in all clones demonstrated a high effective capacity and diversity within the library. The library was then rescued by helper phage M13KO7, with a titer of 10^{12} pfu/mL. Consequently, the titer of the phage display Nb library was determined to be 1.2×10^{12} pfu/mL.

Next, the phage-displayed Nb library was screened using PRMH-BSA as the coating antigen through 4 rounds of affinity panning. The enrichment of PRM-specific phages was observed, and monoclonal strains were selected for identification and screening using ELISA and inhibition calculations (Figure S2). The results demonstrated successful enrichment of phages with higher inhibition rate (inhibition rate>50% at 50 ng/mL), and the range of inhibition rate became more stable with each round of screening. Sequencing of monoclones from each inhibition region (a total of 36) resulted in the acquisition of 7 amino acid sequences, designated as NbFM1~ NbFM7 (Figure 2a). A comparison of these Nb sequences revealed highly conserved FRs regions, while significant variations in the number and type of amino acids were observed in the CDRs regions. In particular, the most diversity in both length and sequence could be observed in CDR3. Among these sequences, NbFM1 and NbFM5 exhibited differences in the number of Cys residues compared to the other sequences.

Expression, purification and Identification of anti-PRM Nbs.

The Nbs above were all expressed in *E. coli* BL21. Then the protein in periplasmic space was extracted by the cold osmotic shock method and then purified using Ni-NTA resin with 200 mmol/L imidazole in 0.01 mol/L PBS for elution[20]. SDS-PAGE analysis of the purified Nbs revealed a protein band slightly higher than 15 kDa, consistent with the expected molecular weight of 18 kDa (Figure 2b). However, the expression levels of Nbs were relatively low, ranging from 0.3 mg/l to 1.8 mg/L (Figure 2c), with NbFM3 exhibiting the highest expression level. The affinity of these Nbs was then evaluated by ELISA and compared with the anti-PRM mAbs (Figure 2d). With the exception of NbFM6 and

NbFM7, all Nbs showed activity at concentrations below 100 ng/mL, indicating a higher antigen-binding capacity compared to the mAbs. In addition, the IC_{50} of the Nbs, except for NbFM7, were below 20 ng/mL, illustrating the high affinity for PRM, particularly NbFM5.

Meanwhile, we performed homology modeling of NbFM5 and NbFM7 using AlphaFold2. The credibility of the models was confirmed by Ramachandran plot map using UCLA-DOE LAB-SAVES v6.0 (Fig. S3). All the models were reasonable when over 95% of amino acids are in the allowable region. which showed that less than 3% of residues of NbFM5/NbFM7 were in the disallowed region (white region). Molecular docking was then conducted between NbFM5/NbFM7 and PRM via LeadIT 2.3.2. The docking result with the lowest score was selected for demonstration (Figure 3).

As shown in Figure 3a–b, PRM was deeply inserted into the active pocket of the CDR3 region in NbFM5, forming a 1.68 Å hydrogen bond with Ala47 and engaging in seven hydrophobic interactions within a 4 Å range (Figure 3c). The analysis of electrostatic potential energy revealed a predominantly negative charge in the pocket, with a strong potential difference near the binding site (Figure 3d). In contrast, the interaction between NbFM7 and PRM appeared weak. Due to sequence diversity, the CDR3 region of NbFM7 was shorter than that of NbFM5, resulting in the formation of a small pocket cavity (Figure 3e), implying the presence of more spatial resistance. Molecular docking further revealed that PRM did not tightly insert into the active pocket of the CDR3 region of NbFM7, while rather on the outer part near the CDR3 region (Figure 3f). The hydrogen bond formed with Cys103 had a bond length of 3.30 Å (Figure 3g) representing a weaker interaction. Besides, fewer hydrophobic bonds were formed within the 4 Å range, and the potential difference was not significant (Figure 3h). These findings indicated that the sequence differences in the CDR3 region of the Nbs would influence the spatial conformation, thereby affecting their interaction with the ligand. Importantly, the benzene ring-containing aspect of PRM was inserted inside NbFM5, while it remained outside in NbFM7, suggesting different binding modes. In summary, NbFM5 was preferentially selected for the development of immunochromatographic assay, while NbFM7 was excluded from further identification attributed to its lowest sensitivity.

Furthermore, the specificity and stability analysis results were performed and presented in Figure S4–5 and Table S2. In summary: (1) the inhibition rate of all Nbs to other analogues was less than 50%; (2) most of the Nbs remained antigen-binding activity after incubation for 1 h and their sensitivity to PRM remained largely unchanged; (3) All Nbs completely lost their activity in the presence of 40% methanol, 20% acetonitrile and 30% acetone, and most of them experienced a loss of at least 20% of their antigen-binding activity in 10% organic solvents. (4) The anti-PRM Nbs exhibited the same acid-base tolerance as mAb and showed better performance, functioning within a pH range of 3.4 ~ 9.4. It is consistent with the previous reports indicating the functional capability of certain Nbs under polar pH conditions[25, 26].

Preparation of btNb and Development of anti-PRM btNb-ICA.

The Nb gene with the highest sensitivity (NbFM5) was cloned from the pComb3X vector into pINQ-BtH6 vector using the *Sfi*I enzyme. The pINQ-BtH6 vector contained a BtAP

receptor peptide with a biotin Avi-tag and a 6xHis-tag, essential for purification, allowing for the biotinylation of NbFM5 under the catalysis of the biotin ligase BirA (Figure 4a). Then the *E. Coli* BL21 (DE3) were transformed with the resulting plasmid for the production of btNb. The expression level of btNb was 4.2 mg/L, higher than that of the non-fusion protein NbFM5 (1.8 mg/L). The biotinylation of NbFM5 was confirmed through SDS-PAGE analysis, which also showed that btNb had a slightly larger molecular weight compared to non-biotinylated NbFM5 due to the specific recognition between the Avi-tag in the pINQ-BtH6 vector and biotin (Figure 4b). ELISA testing further demonstrated that btNb exhibited similar activity and specificity to non-biotinylated NbFM5, indicating no influence on their functional properties. This confirmed that the obtained btNb was suitable for use in the ICA.

Generally, electrostatic adsorption is non-directional and often susceptible to spatial hindrance, whereas labeling with streptavidin allows for the directional labeling of Nbs. This approach enables the rapid functionalization of streptavidin-labeled GNP with btNb, which not only enhances sensitivity through the ultra-high affinity of the biotin-streptavidin system but also allows for reorientation to maximize exposure of Nbs to the analyte, thereby improving Nbs utilization and detection efficiency. Based on this principle, a GNP@SA-btNb was produced using a direct labeling method mediated by biotin-Streptavidin interaction in this work. Then it was utilized for the development of btNb-ICA (Figure 4c), and several parameters were optimized accordingly (Figure S6 and Table S3–5). The detection result could be assessed qualitatively by the naked eye and calculated quantitatively by measuring the T/C value read using a reader. Specifically, in the absence of PRM in the samples, the PRMH-BSA would capture the GNP@SA-btNb, resulting in the formation of a red test line. A negative result would be determined when the T-line was equivalent to that of the C-line. Conversely, the GNP@SA-btNb would preferentially react with free PRM, leading to a negative correlation between the color intensity of the T-line and the concentration of PRM in the samples. The concentration of PRM at which the T-line completely disappeared served as the cut-off value for the test strip. Based on the btNb-ICA mentioned above, several parameters were optimized in a stepwise manner.

The shape and size of GNPs have significant effects on the color development of test strips and detection sensitivity[27]. The uneven shape can lead to system instability, making it easier for proteins bound to the surface to separate, thereby, greatly impacting the labeling results. Fortunately, the GNPs obtained in this study exhibited almost uniform shapes, regardless of their different particle sizes. Besides, the size of GNPs (15 ~ 40 nm) was controlled by adjusting the ratio between chloroauric acid and trisodium citrate (Table S3). The effect of GNPs on the sensitivity of competitive ICA was then investigated (Figure S6a, b). Generally, a smaller GNP diameter results in a significant decrease in overall extinction[28], thereby, reducing the color intensity[29]. Moreover, a larger particle size is positively correlated with color intensity.[28, 29] We found that all probes were significantly more violet than the NbFM5 probe when labeling to SA@btNb. The color intensity was significantly too low when the size was small. As a result, through comprehensive analysis of GNP color, GNP color development degree and the sensitivity on the strip with GNP, the GNP with a particle size of 38 ± 5 nm was selected as the modified carrier for SA to ensure the color development sensitivity of the paper strips. Subsequently, the pH of the GNP solution was adjusted using

K_2CO_3 (Figure S6c, d) to improve the binding efficiency of Nb. However, it was observed in this study that the btNb-ICA agglomerated under the conditions of pH ≤ 8, making it difficult to dissolve after centrifugation and causing it to turn black. While smaller GNPs require higher pH labelling conditions[30], the choice of 38 ± 5 nm GNP to modify Nb was made. Thus, it should be ensured that the reaction takes place under pH > 8. Moreover, the optimal antibody-binding efficiency of streptavidin occurs at pH 9[31]. Hence, btNb was labelled at pH 9 to match this condition.

In competitive ICA, the mass concentration of PRM-BSA detected on the T-line plays a crucial role in determining its color intensity and sensitivity[32]. In the two-step method, both the amount of streptavidin and btNb affected the final binding, and their optimal concentrations were determined (Figure S6e–h). It was observed that the positive inhibition rate decreased as the mass concentration of btNb increase, indicating stable and effective probe conditions (Figure S6e, f). However, when the concentration of btNb decreased to 27.8 μg/mL, the color intensity of the T-line appeared too light, suggesting that the concentration was too low. Similarly, reducing the amount of streptavidin to 16.2 μg/mL did not significantly affect color development and inhibition (Figure S6h), while the GNP and test paper appeared dark purple (Figure S6g), indicating the concentration was too low. Consequently, streptavidin at a concentration of 32.4 μg/mL and btNb at a concentration of 41.7 μg/mL, which exhibited satisfactory color development and sensitivity, were selected for labeling. Furthermore, the usage volume (15 mL per micropore) and concentration (2 mg/mL) of PRMH-BSA on the detection line were further optimized based on negative T/C-line readings and the inhibition rate of the positive solution (Table S4). Finally, the sample pad treatment solution and the diluent for PRM were optimized sequentially (Table S7). The best pad solution consisted of 0.2 mol/L PB buffer containing 0.5% Tween −20, while PB buffer with a pH of 8.4 and ion concentration of 0.2 mol/L was selected as the diluent.

As shown in Figure 4d, the red band on the T-line gradually weakens with the increasing PRM concentration from 0 to 5000 ng/mL, resulting in an IC_{50} value of 6.04 ng/mL and a cut-off value of 200 ng/mL under optimal conditions. The limit of detection (LOD) was 0.88 ng/mL, significantly lower than the national standard limit. Since the national standard limit for PRM is 200 ng/mL, it could be judged qualitatively by naked eye without any instruments and equipment by this method. Moreover, our work offers a simpler and more cost-effective process with minimal batch-to-batch variation compared to previous studies[11, 33]. To validate the stability and reproducibility of the test strip, an accelerated stability experiment was conducted at 45 °C following the method introduced by Liu et al.[34]. The Figure 4e illustrates the signal intensity changes of the negative control strip at different time points. The results indicate that the btNb-ICA retains the color intensity of the C-line color intensity even after 28 days, demonstrating high storage stability and a long shelf life. These favorable developmental characteristics further enhance the reliability of the btNb-ICA method. The specificity of the btNb-ICA method was assessed by analyzing and comparing the chromogenic performance of the test strips with PRM metabolites, 3,5-dichloroaniline, as well as structurally and functionally similar analogs (Figure S6). The results showed that btNb-ICA produced a strong positive reaction only for PRM at a concentration of 20 ng/mL, while showing no significant response to other analogues and

metabolites (20 μg/mL). Thus, it demonstrates that the btNb-ICA developed in this study exhibits high specificity for PRM and can be effectively utilized for specific PRM detection.

Recovery test and instrument validation.

In sample pretreatment, the use of organic solvents is common for extracting hydrophobic drugs to ensure a high extraction rate, while high concentration of organic solvents would disrupt the conformation of antibodies, thus affecting their bioactivity. Nevertheless, this effect could be mitigated through high-magnification dilution or blow-dry redissolution[35]. In this study, chives samples were used for optimization of two treatment methods (direct dilution; dilution after blow-dry and re-dissolution). The acetonitrile extract obtained from the purified chives sample was diluted using QuEChERS method after drying and redissolving. Then the standard curves were fitted under different dilution multiples (Figure 5a, b). Herein, for the purpose of initial screening, a coefficient of variation (CV) of 20% or less is generally acceptable[36, 37]. It was observed that the sensitivity of btNb-ICA decreased under the condition containing 10% acetonitrile (v/v), and the recovery was abnormal at 120%, suggesting a decrease in the bioactivity of btNb. However, when the conditions contained 5% or 2.5% acetonitrile (v/v), the recovery of directly diluted btNb-ICA were 114.6% or 112.4%, higher than those of the same dilution after drying and redissolving. Furthermore, pretreatment with blow-dry and re-dissolution resulted in low recovery, suggesting the loss of some target analytes during the drying process. In summary, a PBS solution with a pH of 8.4 containing 5% acetonitrile (20 times dilution) was selected as the drug diluent for further exploration.

To assess the accuracy and precision of btNb-ICA, a recovery test was performed on samples of chive, cucumber, and tomato using PRM concentrations of 50, 200 and 2000 μg/kg. The results presented in Table 1 showed that the recoveries of btNb-ICA ranged from 82.2% to 117.3%, with CV values ranging from 2.6% to 14.6%. These low CV values indicated the excellent reproducibility of btNb-ICA. The acceptable recoveries and CV values confirmed that the btNb-ICA was suitable for rapid on-site detection and quantitative analysis of PRM. Furthermore, four randomly labeled chive, cucumber and tomato samples were compared by btNb-ICA and GC-MS/MS. The results, as depicted in Figure 5c, revealed a good correlation between btNb-ICA and GC-MS/MS, with a correlation coefficient of 0.995. Consequently, the btNb-ICA established in this study provides accurate quantitative detection of PRM.

Besides, Nb has the advantage of high solubility and efficient expression in large quantities, resulting in lower time and production costs compared to traditional antibodies used in other studies[11, 33]. Furthermore, due to the higher organic tolerance of nanobodies, the sample pretreatment procedures of drying and redissolving with organic solvent can be omitted, resulting in significant time and cost savings. Meanwhile, the higher tolerance of nanobodies to sample matrix and organic solvents also ensures that the matrix effect has minimal impact on the performance of nanobodies. This increased robustness allows for more accurate and reliable detection of PRM in fruits and vegetables in agricultural markets. In summary, the developed btNb-ICA provides a rapid, specific and accurate method for the detection of

PRM in fruits and vegetables in the agricultural markets. The high specificity and accuracy make it a suitable choice for ensuring food safety and quality control.

Supplementary Material

Refer to Web version on PubMed Central for supplementary material.

Acknowledgments

This work was supported by the National Key Research and Development of China (2019YFE0116600), Guangdong Provincial Science and Technology Project, China (2022A0505050061), Guangdong Basic and Applied Basic Research Foundation (2021A1515110513) and the Guangdong Special Support Program, China (2019TX05N052). Partial support was provided by NIH-NIEHS (RIVER Award) R35 ES030443-01 and NIH-NIEHS (Superfund Award) P42 ES004699.

Data availability

Data will be made available on request.

ABBREVIATIONS

PRM	procymidone
Nbs	nanobodies
CDR3	complementarity-determining region 3
ICA	immunochromatographic assay
btNb	biotinylated Nb
LOD	limit of detection
IC_{50}	half-inhibitory concentration
MRLs	maximum residue limits
ic-ELISA	indirect competitive enzyme-linked immunosorbent assay
VHH	the variable domain of the heavy-chain of heavy-chain antibody
FRs	framework regions
btNb-ICA	gold-labeled immunochromatographic assay based on btNb
GNP	gold nanoparticle
GNP@SA	streptavidin labeled GNP
T-line	test line
C-line	control line

References:

(1). Zhang S; Li L; Meng G; Zhang X; Hou L; Hua X; Wang M, Environmental behaviors of procymidone in different types of Chinese soil. Sustainability-Basel. 2021, 13, (12), 6712.

(2). Li L; Zhao T; Liu Y; Liang H; Shi K, Method validation, residues and dietary risk assessment for procymidone in green onion and garlic plant. Foods. 2022, 11, (13), 1856. [PubMed: 35804675]

(3). Kapukıran F; Fırat M; Chormey DS; Bakırdere S; Özdoğan N, Accurate and sensitive determination method for procymidone and chlorflurenol in municipal wastewater, medical wastewater and irrigation canal water by GC-MS after vortex assisted switchable solvent liquid phase microextraction. B. Environ. Contam. Tox 2019, 102, (6), 848–853.

(4). Lai Q; Sun X; Li L; Li D; Wang M; Shi H, Toxicity effects of procymidone, iprodione and their metabolite of 3,5-dichloroaniline to zebrafish. Chemosphere. 2021, 272, (8), 129577. [PubMed: 33465616]

(5). National food safety standard-maximum residue limits for pesticides in food[S]. In GB2763–2021. 2021.

(6). National food safety standard-maximum residue limits for 112 pesticides in food[S]. In GB 2763.1-2022. 2022.

(7). Pesticide MRLs in food-procymidone[S]. In Ministry of Food and Drug Safety. 2017, p 689.

(8). AB2018-Maximum residue limits (MRLs) list of agricultural chemicals in foods-procymidone[S]. In Ministry of Health, Labor and Welfare of Japan. 2018.

(9). Environmental Protection Agency (EPA), Protection of Environment. In Code of Federal Regulations. 2014, pp 169–171.

(10). Wang W; Gao Z; Qiao C; Liu F; Peng Q, Residue analysis and removal of procymidone in cucumber after field application. Food Control. 2021, 128, (1), 108168.

(11). Fernandez-Alba AR; Valverde A; Agüera A; Contreras M; Rodriguez D, Determination of procymidone in vegetables by a commercial competitive inhibition enzyme immunoassay. Anal. Chim. Acta 1995, 311, (3), 371–376.

(12). Lefranc M; Lefranc G, IMGT® and 30 years of immunoinformatics insight in antibody V and C domain structure and function. Antibodies (Basel). 2019, 8, (2), 29. [PubMed: 31544835]

(13). Salvador JP; Vilaplana L; Marco MP, Nanobody: outstanding features for diagnostic and therapeutic applications. Anal. Bioanal. Chem 2019, 411, (9), 1703–1713. [PubMed: 30734854]

(14). Qin Q; Liu H; He W; Guo Y; Zhang J; She J; Zheng F; Zhang S; Muyldermans S; Wen Y, Single domain antibody application in bacterial infection diagnosis and neutralization. Frontiers in Immunology. 2022, 13, 1014377.

(15). Wang J; Mukhtar H; Ma L; Pang Q; Wang X, VHH antibodies: reagents for mycotoxin detection in food products. Sensors-Basel. 2018, 18, (2), 485. [PubMed: 29415506]

(16). Wang Y; Zhang C; Wang J; Knopp D, Recent progress in rapid determination of mycotoxins based on emerging biorecognition molecules: a review. Toxins. 2022, 14, (2), 73. [PubMed: 35202100]

(17). Srinivasan L; Alzogaray V; Selvakumar D; Nathan S; Yoder JB; Wright KM; Klinke S; Nwafor JN; Labanda MS; Goldbaum FA; Schön A; Freire E; Tomaselli GF; Amzel LM; Ben-Johny M; Gabelli SB, Development of high-affinity nanobodies specific for NaV1.4 and NaV1.5 voltage-gated sodium channel isoforms. J. Biol. Chem 2022, 298, (4), 101763. [PubMed: 35202650]

(18). Hu Y; Wang Y; Nie L; Lin J; Wu S; Li S; Wu J; Ji X; Lv H; Muyldermans S; Wang S, Exploration of specific nanobodies as immunological reagents to detect milk allergen of β-lactoglobulin without interference of hydrolytic peptides. J. Agr. Food Chem 2022, 70, (48), 15271–15282. [PubMed: 36412552]

(19). Hu Y; Lin J; Peng L; Wang Y; Wu S; Ji X; Lv H; Wu J; Zhang Y; Wang S, Nanobody-based electrochemical immunoassay for sensitive detection of peanut allergen ara h 1. J. Agr. Food Chem 2023, 71, (19), 7535–7545. [PubMed: 37158222]

(20). Chen Z; Zhang Y; Chen J; Lin Z; Wu M; Shen Y; Luo L; Wang H; Wen X; Hammock B; Lei H; Xu Z, Production and characterization of biotinylated anti-fenitrothion nanobodies and development of sensitive fluoroimmunoassay. J. Agr. Food Chem 2022, 70, (13), 4102–4111. [PubMed: 35333506]

(21). Fu H; Wang Y; Xiao Z; Wang H; Li Z; Shen Y; Lei H; Sun Y; Xu Z; Hammock B, A rapid and simple fluorescence enzyme-linked immunosorbent assay for tetrabromobisphenol A in soil samples based on a bifunctional fusion protein. Ecotox. Environ. Safe 2020, 188, 109904.

(22). F. G, Controlled nucleation for the regulation of the particle size in monodisperse gold suspensions. Nature. 1973, 241, (105), 20–22.

(23). National food safety standard-determination of 208 pesticides and metabolites residues in foods of plant origin gas chromatography-tandem mass spectrometry method[S]. In GB 23200.113-2018. 2018.

(24). Kulkarni SS; Falzarano D, Unique aspects of adaptive immunity in camelids and their applications. Mol. Immunol 2021, 134, 102–108. [PubMed: 33751993]

(25). Petersson M; Thrane SW; Gram L; Muyldermans S; Laustsen AH, Orally delivered single-domain antibodies against gastrointestinal pathogens. Trends Biotechnol. 2023, 41, (7), 875–886. [PubMed: 36774206]

(26). Ren J; Xiong H; Huang C; Ji F; Jia L, An engineered peptide tag-specific nanobody for immunoaffinity chromatography application enabling efficient product recovery at mild conditions. J. Chromatogr. A 2022, 1676, 463274. [PubMed: 35780707]

(27). Shao Y; Xu W; Zheng Y; Zhu Z; Xie J; Wei X; Zhang Y; Zhang J; Wu Q; Wang J; Ding Y, Interface coordination achieving excellent optical properties of three-dimensional dendritic gold nanoparticles for immunochromatographic performance. Chem. Eng. J 2023, 455, 140586.

(28). Khlebtsov BN; Tumskiy RS; Burov AM; Pylaev TE; Khlebtsov NG, Quantifying the numbers of gold nanoparticles in the test zone of lateral flow immunoassay strips. ACS Applied Nano Materials. 2019, 2, (8), 5020–5028.

(29). Chotithammakul S; Cortie MB; Pissuwan D, Comparison of single- and mixed-sized gold nanoparticles on lateral flow assay for albumin detection. Biosensors. 2021, 11, (7), 209. [PubMed: 34206883]

(30). Lou S; Ye J; Li K; Wu A, A gold nanoparticle-based immunochromatographic assay: the influence of nanoparticulate size. Analyst (London). 2012, 137, (5), 1174–1181. [PubMed: 22193208]

(31). Thobhani S; Attree S; Boyd R; Kumarswami N; Noble J; Szymanski M; Porter RA, Bioconjugation and characterisation of gold colloid-labelled proteins. J. Immunol. Methods 2010, 356, (1–2), 60–69. [PubMed: 20188107]

(32). Zhang J; Ruan H; Wang Y; Wang Y; Ke T; Guo M; Tian J; Huang Y; Luo J; Yang M, Broad-specificity monoclonal antibody against neonicotinoid insecticides via a multi-immunogen strategy and development of a highly sensitive GNP-based multi-residue immunoassay in ginseng and tomato. Food Chem. 2023, 420, 136115. [PubMed: 37062080]

(33). Li G; Sun J; Li J; Zhang Y; Huang J; Yue F; Dong H; Li F; Xu H; Guo Y; Guo Y; Sun X, Paper-based biosensors relying on core biological immune scaffolds for the detection of procymidone in vegetables. Talanta 2023, 265, 124843. [PubMed: 37399648]

(34). Liu Z; Hua Q; Wang J; Liang Z; Zhou Z; Shen X; Lei H; Li X, Prussian blue immunochromatography with portable smartphone-based detection device for zearalenone in cereals. Food Chem. 2022, 369, 131008. [PubMed: 34500205]

(35). Dzantiev BB; Byzova NA; Urusov AE; Zherdev AV, Immunochromatographic methods in food analysis. Trends Analyt. Chem 2014, 55, 81–93.

(36). Yu F; Wu Y; Yu S; Zhang H; Zhang H; Qu L; Harrington PDB, A competitive chemiluminescence enzyme immunoassay for rapid and sensitive determination of enrofloxacin. Spectrochim. Acta A Mol. Biomol. Spectrosc 2012, 93, 164–168. [PubMed: 22472132]

(37). Stove V; Ramos PA; Wallemacq P; Vogeser M; Schuetzenmeister A; Schmiedel C; Shipkova M, Measurement of sirolimus concentrations in human blood using an automated electrochemiluminescence immunoassay (ECLIA): a multicenter evaluation. Clin. Chem. Lab. Med 2018, 56, (5), 764–775. [PubMed: 29206642]

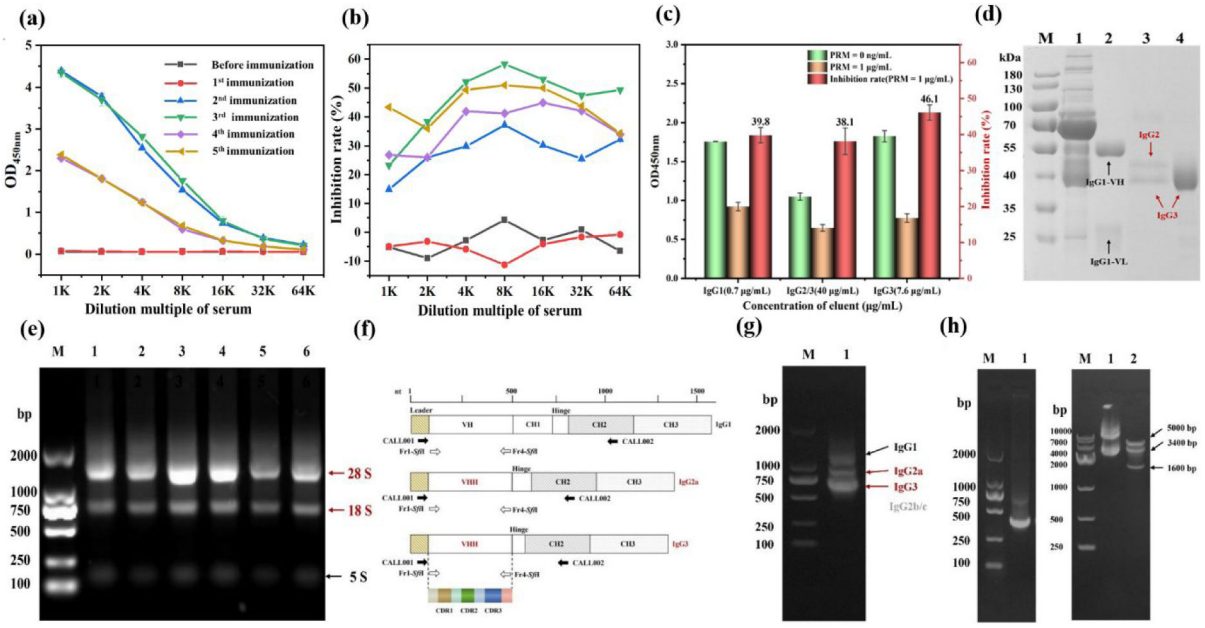

Figure 1.

Identification of serum subtypes isolated from serum in Bactrian camels and construction of Nb genes library. (a) Curves of antigen-binding capacity; (b) Curves of inhibition rate; (c) Isolation and identification of serum subtypes in Bactrian camels; (d) SDS-PAGE of serum subtypes. M: marker; 1: serum; 2: IgG_1 elution; 3: IgG_2 elution; 4: IgG_3 elution; (e) Extraction of the total RNA; (f-g) The amplification of the VHH genes; (h) The second round of PCR and the digestion of pcomb3xSS.

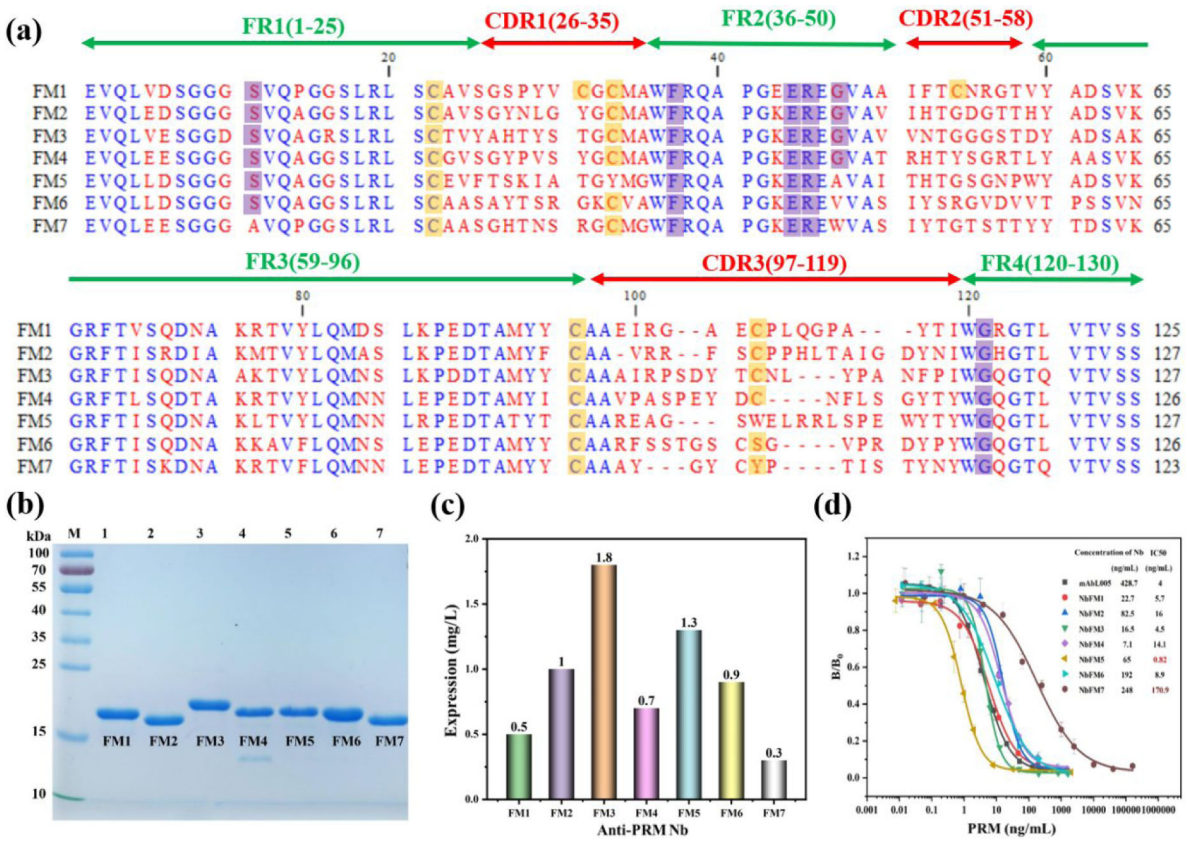

Figure 2.

Identification of Nbs with different sequences. (a) amino acid sequences of NbFM1 ~ NbFM7; (b) SDS-PAGE; (c) The amount of expression; (d) Identification of NbFM1 ~ NbFM7 by ic-ELISA.

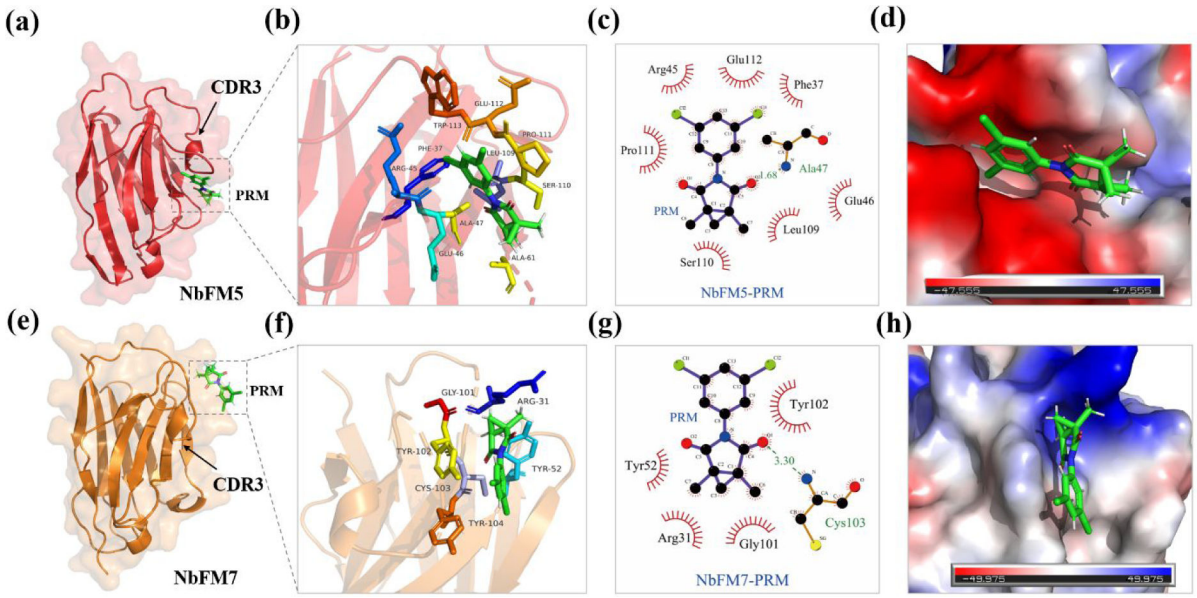

Figure 3.

Molecular docking between PRM and anti-PRM NbFM5/NbFM7. (a-b) The docking results between NbFM5 and PRM; (c) The interaction forces between NbFM5 and PRM; (d) The electrostatic potential energy generated by NbFM5-PRM; (e-f) The docking results between NbFM7 and PRM; (g) The interaction forces between NbFM7 and PRM; (h) The electrostatic potential energy generated by NbFM7-PRM.

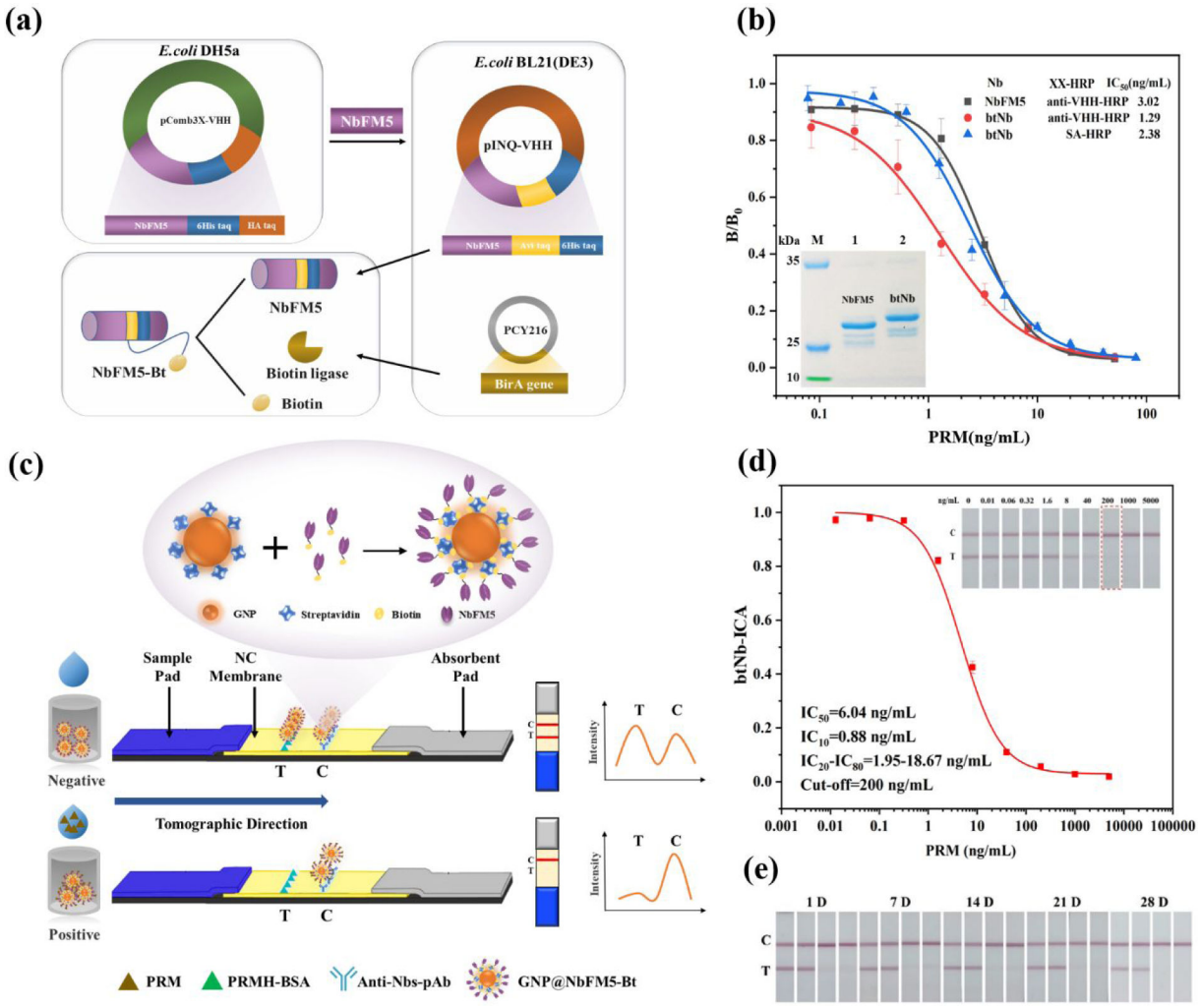

Figure 4.

Preparation of btNb and development of btNb-ICA; (a) Directed biotinylated gene design principle; (b) Directed btNb preparation and identification curve; M: Marker; 1: NbFM5; 2: btNb; (c) The principle of targeted labeling of anti-PRM btNb and detection of btNb-ICA; (d) The calibration curves of the btNb-ICA; (e) The stability test in 45°C of the btNb-ICA.

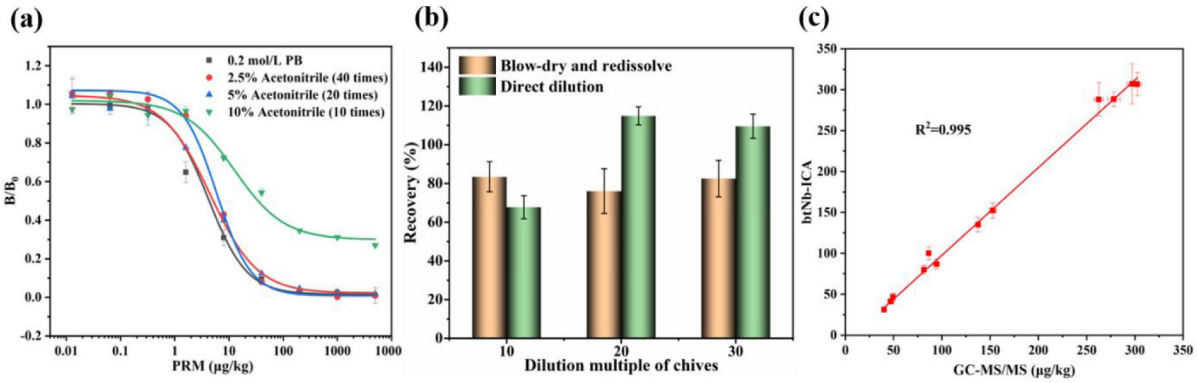

Figure 5.

Optimization of extraction method and the sensitivity of btNb-ICA. (a) The effect of acetonitrile content in direct dilution pretreatment on detection sensitivity based on btNb-ICA; (b) The influence of different sample pretreatment methods on the recoveries of btNb-ICA; (c) The accuracy of btNb-ICA was verified by GC-MS/MS (n=3).

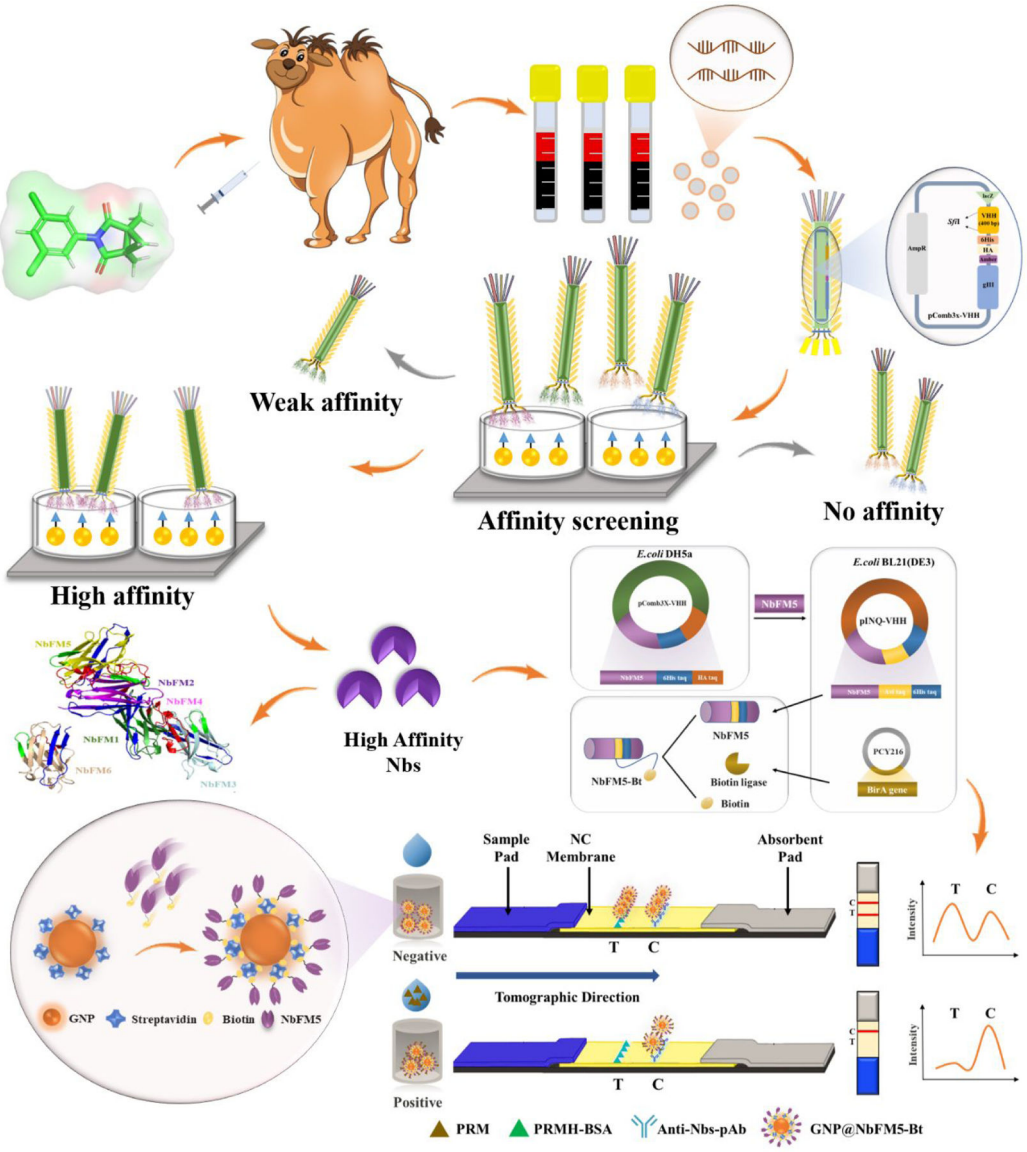

Scheme 1.

Preparation of anti-PRM Nbs and development of immunochromatography. (Number of animal ethical review certificate: 2020f064)

Table 1

Recovery Test Results of Sample Addition for btNb-ICA (n=3).

Samples	Addition value (μg/kg)	Measured values (X±SD) (μg/kg)	Recovery (%)	CV (%)
Chives	50	46.7±4.5	93.5	9.6
	200	172.9±11.7	86.5	6.8
	2000	1698.8±100.6	84.9	5.9
Cucumbers	50	41.1±3.4	82.2	8.1
	200	169.6±24.7	84.8	14.6
	2000	2338±205.7	116.9	8.8
Tomatoes	50	50.1±3.4	100.3	6.9
	200	210.8±5.6	105.4	2.6
	2000	2346.7±116.5	117.3	5.0